Journal of Building Engineering 76 (2023) 107203

Contents lists available at ScienceDirect

Journal of Building Engineering

journal homepage: www.elsevier.com/locate/jobe

The strength of beam-to-RHS joints with welded studs

Ismael García *, Miguel A. Serrano, Carlos López-Colina, Fernando L. Gayarre

University of Oviedo, Dep. Construction and Manufacturing Engineering, Campus Gijón, 33203, Spain

ARTICLE INFO

Keywords:
Tubular structures
Welded studs
Bolted connections
Joint characterization
Sustainable construction
Component method

ABSTRACT

Construction industry is a significant contributor to global warming and other impacts on the environment. Demountable building may be a key to achieve sustainable construction as it facilitates the separation of components and materials for their recovery or even their reuse. However, when designing demountable bolted beam-to-column joints involving IPE-beams and hollow sections columns, difficulties associated with the inaccessibility of the interior of the tube can result in a problem during the execution process. To solve this problem, the use of joints with welded studs is great of interest since threaded studs can be attached to the column face without accessing the inside of the tube. The threaded studs can be used in combination with angle cleats to assembly demountable joints. In this paper, a new component-based analytical model to determine the resistance of beam to column bolted joints is presented. Firstly, analytical equations to calculate the resistance of the studs are proposed. Then their assessment with experimental tests is evaluated. Finally, the analytical strength and failure modes of the full joint are compared with the results obtained in a vast campaign of full-scale experimental tests, including single-side bolted beam-column joints and double-side bolted beam-column joints. The design parameters that govern the resistance of the full joints were also revealed. Drawing on this knowledge, guidelines to the design of joints based on their expected behavior have been proposed.

1. Introduction

Construction industry plays an important role in overall energy consumption with buildings account for 40% of total energy consumption in the European Union [1]. Construction activity consumes energy in many ways, such as using heavy machinery, transportation of materials, and operation of lighting and heating systems. Additionally, the manufacturing process of building materials, such as cement and steel, also needs a high amount of energy and are one of the most significant sources of CO_2 emissions, producing 7% [2] and 6.7% [3] of worldwide emissions respectively. Reducing CO_2 emissions in these industries is one of the most important challenge the world will face in the coming decades [4]. The energy consumption during the construction phase of a building has a significant impact on its overall environmental footprint. Many research studies [5] have focused on the emissions produced from the construction materials during the manufacturing, execution, replacement, and end-of-life stages.

Reducing construction and demolition waste through recycling and reuse may contribute to decrease CO_2 emissions [6]. Although the capacity of reuse and recycle of welded steel buildings are notably lower than those of other construction technologies, welded joints generally imply higher stiffness and resistance [7–9]. In contrast, the use of bolted joints makes it possible to disassemble the joints and facilitates increased flexibility and adaptability to new scenarios. Furthermore, as the members can be demounted, the

* Corresponding author.
E-mail address: garciaismael@uniovi.es (I. García).

https://doi.org/10.1016/j.jobe.2023.107203
Received 20 March 2023; Received in revised form 7 June 2023; Accepted 26 June 2023
Available online 28 June 2023

buildings can be disassembled and deconstructed [10] allowing an efficient separation of components and materials for their recovery and their reuse. This is expected to contribute to a more environmentally responsible building life cycle [11,12].

The design of bolted joints with structural hollow sections presents challenges as the placement of bolts within the inner part of the hollow sections can hinder the assembling due to the inaccessibility of the interior. In the last years, some authors have studied the use of bolted joints connecting hollow steel columns and I-beams. Málaga-Chuquitaype et al. [13,14] proposed the use of blind bolts that only requires accessing from one side of the hollow structural section. Another alternative was proposed by Málaga-Chuquitaype et al. [15] and Liu et al. [16–18] who proposed a kind of connection which requires a channel and an end plate or an angle cleat as intermediate pieces. In these joints, the channel must be previously welded to the column. An option that makes the joint demountable, when using concrete-filled tubular columns and does not require intermediate pieces, is the use of threaded welded studs. This technique, which only requires welding threaded studs to the frontal face of the hollow section by using a simple stud welding gun, was initially proposed in the CIDECT 5AG project by Maquoi [19,20] and later has been studied by Vandegans et al. [21–23], Neves et al. [24] and Serrano et al. [25–27].

Arc stud welding is an electric arc process that consists of welding a stud to a base metal. The stud can adopt many shapes: threaded, unthreaded, square, etc. Both the stud and the base metal can be made of various materials including steel, stainless steel, aluminium etc. In arc stud welding, the stud is attached to the workpiece without accessing the other side of the base plate, which made the process suitable in the design of joints with hollow-section profiles.

In this paper, the resistance of beam-column bolted joints formed by tubular columns and open-section beams (Fig. 1) is studied. These joints are designed to be demountable and with reusability in mind. The joints are executed by means of threaded studs welded to the face of the column. The studs connect the column with the short leg of the top and seat angle cleats, while the long leg of the angle cleats is connected to the beam flanges by using standard bolts, as it can be seen in Fig. 1. The use of angle cleats avoids the issue when working with end-plate connections and welded studs as the assembly is extremely complex for single-piece beams. Hydraulic jacks would need to be used to increase the gap between columns beyond the length of the connectors in order to position the beam between two columns.

Eurocode 3 (1.8) [28] provides guidelines for determining the stiffness and strength of various types of joints using the component method. This approach classifies joints based on their rotational stiffness (pinned, semi-rigid, and rigid) and their moment resistance (pinned, partial-strength, and full-strength). Despite its usefulness and versatility, the component method was initially developed for joints involving open-section profiles and does not cover joints formed by open-section beams and hollow-section columns, in its standardized application proposals. To fill this gap, this paper proposes an analytical model that can accurately depict both the strength and failure modes of IPE-beam to hollow section joints with welded studs through the component-based approach. To this aim, the resistance of the basic components has been calculated using adapted equations from Eurocode 3 where feasible, while for the tube's key components new equations have been proposed. The results of the analytical component-based model were compared to those obtained from full-scale experimentally tested joints with a high level of consistency. Finally, guidelines for designing this type of joints with welded studs are proposed.

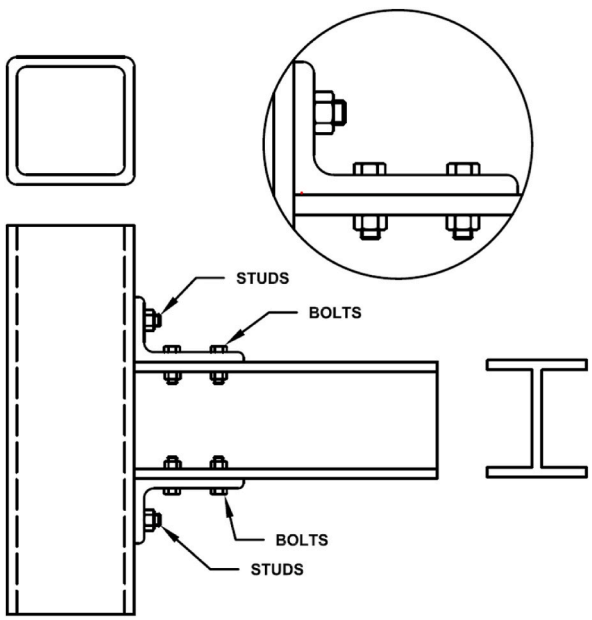

Fig. 1. Example of an I-beam to tubular column joint with unequal sided top and seat angle cleats and welded studs.

2. Experimental program

Twelve full-scale hollow section-column to I-beam bolted joints with double angle cleat were used to determine their moment-rotation curves from which the ultimate moment resistances have been obtained. A failure analysis of the joint allowed to identify the root mode of failure of the joints. The results obtained through the experimental moment-rotation curves were used to validate the analytical equations proposed to easily obtain the resistance of the whole joint. Furthermore, welded studs were subjected to tensile and shear loads in order to validate the analytical equations for the resistance of the studs.

2.1. Beam-to-column experimental program

For the experimental evaluation of the resistance of the beam-to-column joints with welded studs, two different types of joints were considered: a) a beam connected to one side of the column (denoted as SMS here) and b) beams connected to both sides of the column (coded as DMS). The SMS and DMS test configurations were selected based on the two possible joint situations that can arise when the joints are part of a framed structure. Specifically, the SMS configuration corresponds to the case of a beam-column connection in which the column is a corner column. The DMS configuration would be appropriate for an intermediate column joint. It is important to highlight a significant difference between these two configurations. In SMS joints, the lateral face experiences shear forces, while this does not occur in DMS joints. An example of each type of joint can be seen in Fig. 2. The detailed experimental study was published by the authors in a previous paper [25].

The SMS joints consist of either a square (SHS) or rectangular (RHS) hollow section column with a length of 900 mm, and a beam with a cross-section HEB 200 or IPE 300 and length of 840 mm. Beam and column are joined together by angle cleats of unequal sides type L 120x80x10, which connect the flanges of the beam to the frontal face of the column. The angle cleats are fixed to the beam by metric threaded bolts of M16 and class 8.8, and to the column by welded threaded studs with a reduced diameter on the non-threaded area, with a metric thread M16, class K800 (8MnSi7) and 40 mm in length. The various beam-to-column joint configurations for one side are presented in Table 1 (specimens SMS), with the relationship between the beam width and the column width, denoted as parameter β, shown in the last column.

The DMS joints consist of either a square (SHS) or rectangular (RHS) hollow section column with a length of 900 mm and two HEB 200 or IPE 300 beams with a length of 470 mm, joined together by four angles of unequal sides L 120x80x10. These sections were used to study joints with a beam width to column width ratio of $\beta = 1$ and $\beta = 0.75$. The angle cleats are connected to the flanges of the beams by metric 16 mm 8.8 bolts, and to the column by welded threaded studs of reduced diameter in the non-threaded area. The studs were 16 mm in diameter, grade 4.8 (S235), and 35 mm in length. The various beam-to-column joint configurations with beams on both sides of the column are presented in Table 1.

Table 2 shows the dimensions of the studs as they correspond to the geometric parameters illustrated in Fig. 3. As it can be seen in the figure, the studs were threaded studs but with reduced area (RD studs). This means this type of studs presents less diameter in the unthreaded section than in the threaded part. A ceramic ferrule RF16 was used to protect the molten weld pool. Fig. 4 shows the geometry of the angle cleats, including the location of the holes. The distance of the holes from the edge was chosen in accordance with the minimum and maximum distances specified by Eurocode 3 (1.8) [28]. The bolts were tightened using a torque of 190 Nm, executed in two stages. First, a torque of 150 Nm was applied, followed by a second stage where the bolts were tightened to 190 Nm.

The experimental results for the joint resistance are presented later to be compared with those obtained by means of the analytical proposal.

2.2. Tensile stud testing

M16 and M20 studs were welded to structural tubes to determine their resistance when the studs are subjected to tensile loads. To carry out the test, two studs with the same diameter were welded in a symmetrical position on the two opposite faces of the tube and a tensile load was applied to the studs until failure occurred. In these tests, two diameters of 16 mm and 20 mm are considered combined with two classes of studs: 4.8 and K800. Each different type of stud was welded to three different tube thicknesses of 6, 8 and 10 mm, in a set of twelve specimens shown in Fig. 6.

Table 3 shows the maximum load from the test, $F_{u,exp}$, for each stud-tube assembly based on stud diameter, quality of the stud, and

Fig. 2. Type of beam-column joints tested. (a) Beam connection to one side of the column (SMS); (b) Connection with beam on both sides of the column (DMS).

Table 1
Set-up of the beam-column joints tested with beam on one side (SMS) and beam on both sides (DMS).

Specimen	Column + Beam	No. of Angle cleats L120 × 80 × 10	Bolts	Studs	B [b_b/b_0]
SMS1	SHS 200.6 + HEB 200	2	8 × M16 8.8	4 M16 × 40 K800	1
SMS2	SHS 200.8 + HEB 200	2	8 × M16 8.8	4 M16 × 40 K800	1
SMS3	SHS 200.10 + HEB 200	2	8 × M16 8.8	4 M16 × 40 K800	1
SMS4	SHS 200.6 + IPE 300	2	8 × M16 8.8	4 M16 × 40 K800	0.75
SMS5	SHS 200.8 + IPE 300	2	8 × M16 8.8	4 M16 × 40 K800	0.75
SMS6	SHS 200.10 + IPE 300	2	8 × M16 8.8	4 M16 × 40 K800	0.75
SMS7	RHS 200.150.6 + IPE 300	2	8 × M16 8.8	4 M16 × 40 K800	1
SMS8	RHS 200.150.8 + IPE 300	2	8 × M16 8.8	4 M16 × 40 K800	1
SMS9	RHS 200.150.10 + IPE 300	2	8 × M16 8.8	4 M16 × 40 K800	1
DMS1	SHS 200.8 + HEB 200	4	16 × M16 8.8	8 M16 × 35 4.8	1
DMS2	SHS 200.6 + IPE 300	4	16 × M16 8.8	8 M16 × 35 4.8	0.75
DMS3	SHS 200.8 + IPE 300	4	16 × M16 8.8	8 M16 × 35 4.8	0.75
DMS4	RHS 200.150.8 + IPE 300	4	16 × M16 8.8	8 M16 × 35 4.8	1

Table 2
Geometric properties of studs.

d_1	class	l_2 [mm]	d_2 [mm]	d_3 [mm]	y_{min} [mm]	h_1 [mm]	Ceramic ferrule
M16	K800 (8Mnsi7)	40	13.2	18	11	6	RF16
M16	4.8 (S235)	35	13.2	18	11	6	RF16

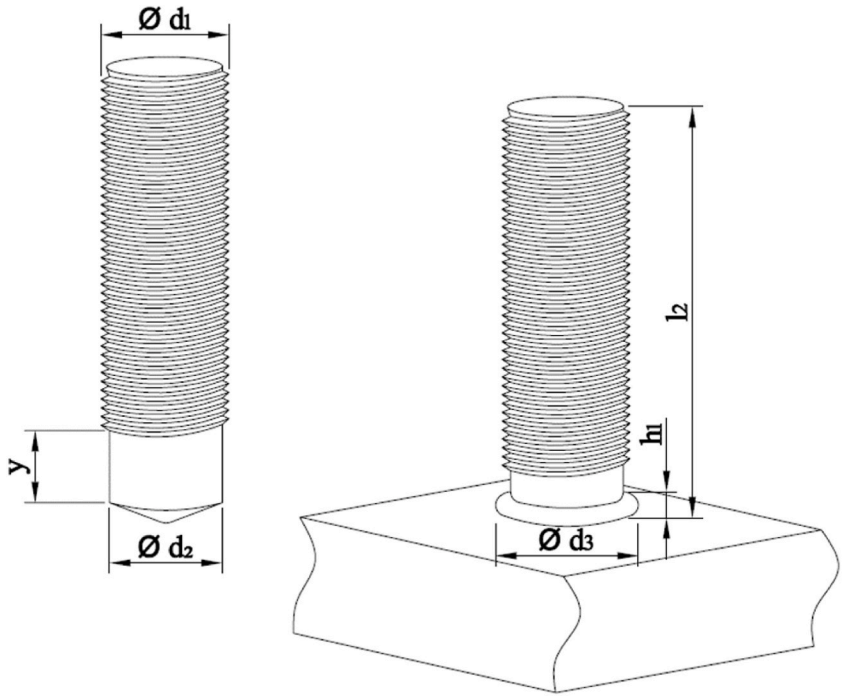

Fig. 3. Geometric parameters of the threaded studs with reduced diameter: before welding (left) and after welding (right).

the thickness of the tube. In the instance of tubes with a thickness of 6 mm, the failure mode resulted from the punching of the stud on the frontal face of the tube. For thicker tubes, the failure was primarily due to tension on the studs. However, in some assemblies with a tube thickness of 8 mm, the failure resulted from a combination of both modes.

2.3. Shear stud testing

The aim of this section is to describe the experimental tests to obtain the resistance of welded studs under shear to later correlate the results with the analytical predictions.

Six specimens were prepared to obtain the resistance of the studs under shear. The thicknesses of the specimens were selected following the NASM1312-13 standard practise for double shear test while the rest of the dimensions were selected with the dimensions

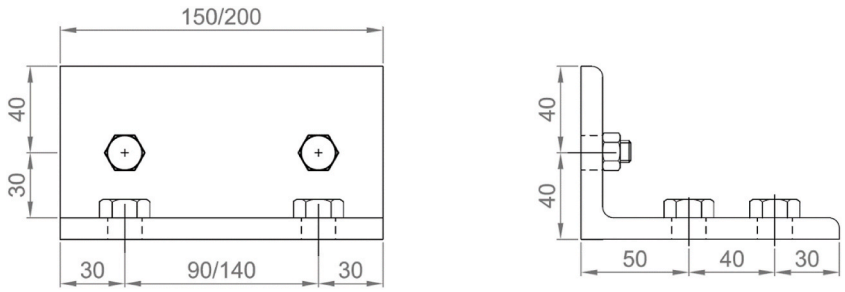

Fig. 4. Geometry of the angle cleats and position of the holes in the beam-to-column joints.

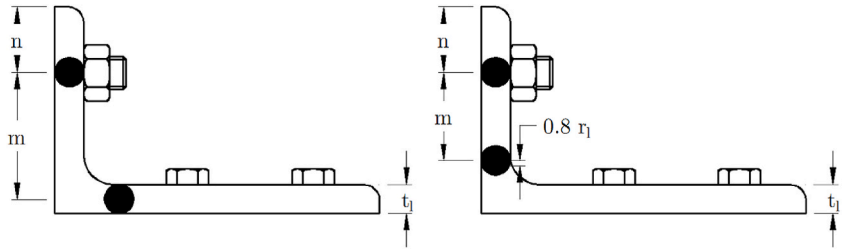

Fig. 5. Definition of the m-parameter, variable with the distance between the beam and the column. When the distance is higher than 0.4 t_l (left) and when the distance is lower or equal to 0.4 t_l (right).

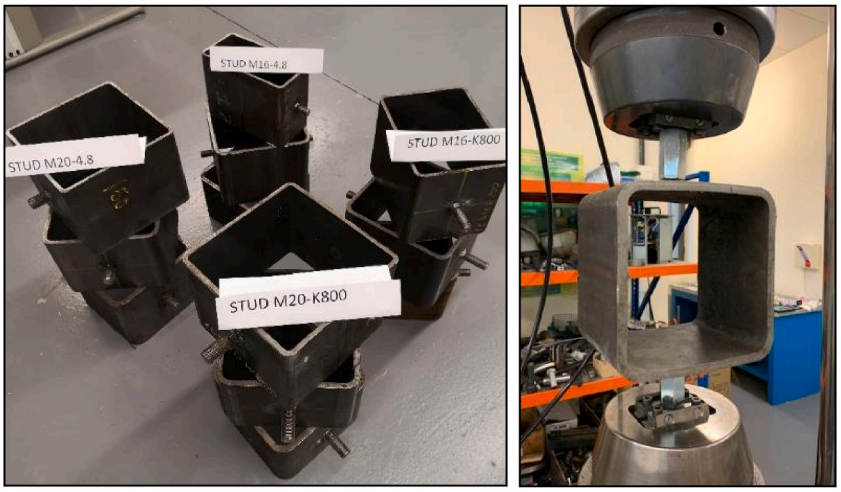

Fig. 6. Welded studs under tensile tests. Studs welded to structural tubes (left) and general set-up of the test (right).

proposed in Annex G of UNE-EN 1090-2:2019 standard. The specimens used in the shear tests consisted of a steel plate in which two studs with diameters of 16-mm or 20-mm were welded on both faces of the plate (Figs. 7 and 8). The steel grades of the studs were 4.8 and K800 and two options regarding the dimensions of the hole to accommodate the weld collar were considered. Thus, counterbored specimens, to make wider the side of the hole in which the collar weld is located and specimens with a constant diameter in the holes were tested.

To carry out the tests, two double shear test configurations were considered due to the load capacities of the available testing machines and the options of gripping systems on each of the machines. In this way, the tests of the M20 studs, for which a greater load capacity was expected, were carried out under compression using a hydraulic actuator from the firm Ibertest, with a load capacity of 750 kN. The tests of the M16 studs were carried out under tension in a universal testing machine from the MTS firm equipped with hydraulic wedge grips and with a load capacity of 250 kN.

In both configurations two studs with the same geometry and aligned with each other were welded on the opposite faces of a plate with the same thickness as the diameter of the stud. A pair of additional steel plates with half the thickness of the intermediate plate were attached to each side of the thicker plate. The dimensions of the specimens with M16 studs are shown in Fig. 7 while the

Table 3
Results of the tests of the studs under tensile.

Specimen	Experimental		Analytical				
	t_0 [mm]	$F_{u,exp}$ [kN]	$F_{t,Rd}$ [kN]	$B_{p,Rd}$ [kN]	$F_{lt,Rd}$ [kN]	$R_{s,Rd}$ [kN]	$\frac{F_{u,exp}}{R_{s,Rd}}$
S16–4.8	5.54	51.1	62.2	51.5	62.3	51.5	0.99
S16–4.8	7.62	73.7	62.2	70.9	62.3	62.2	1.18
S16–4.8	9.76	75.2	77.8	104.6	68.7	68.7	1.09
S16–K800	5.58	54.3	79.2	54.2	64.2	54.2	1.00
S16–K800	7.62	71.6	79.2	74.0	64.2	64.2	1.12
S16–K800	9.77	–	65.8	104.0	68.4	65.8	-
S20–4.8	5.66	43.3	97.2	65.8	97.4	65.8	0.66
S20–4.8	7.62	83.8	97.2	88.6	97.4	88.6	0.95
S20–4.8	9.76	119.8	121.6	130.7	107.4	107.4	1.12
S20–K800	5.66	47.1	101.8	67.0	98.6	67.0	0.70
S20–K800	7.75	–	101.8	91.8	98.6	91.8	–
S20–K800	9.77	121.1	119.3	130.1	106.9	106.9	1.13

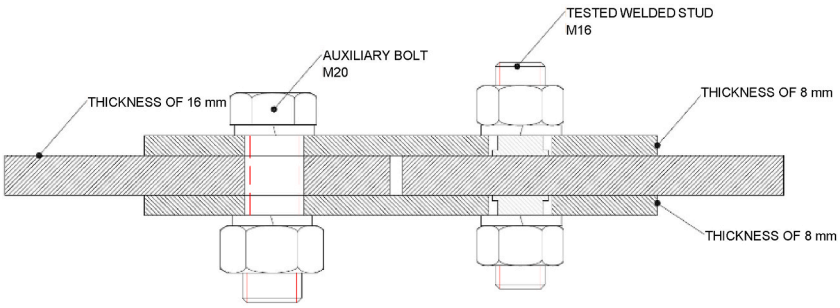

Fig. 7. Details of the specimens with M16 studs under shear.

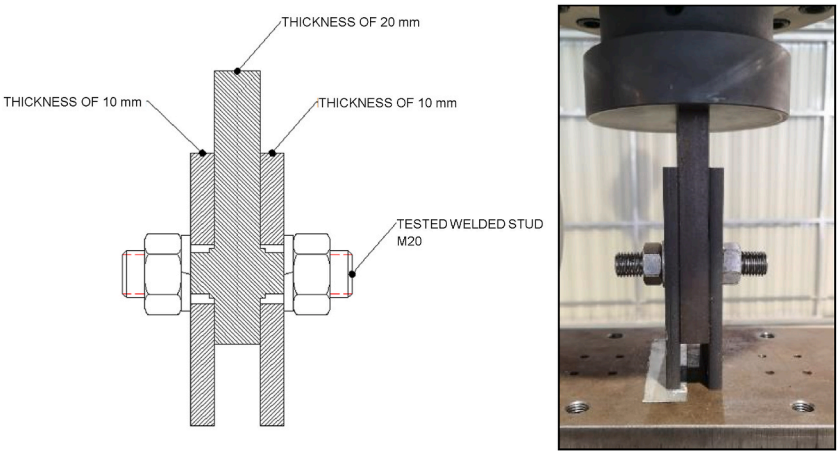

Fig. 8. Details of the specimens with M20 studs under shear: dimensions of the specimens (left) and scheme of the load application procedure (right, shown in perspective).

dimensions of the specimens with M20 studs are shown in Fig. 8. As it can be seen in Fig. 7, the external steel plates in specimens with M16 studs were fixed to the intermediate steel plate by using an auxiliar standard bolt M20 and steel grade of 8.8. These tests in tension were carried out under displacement control at a rate of 1 mm/min. In M20 specimens, the steel plates were shorter and thicker than in the M16 specimens to avoid instabilities. The M20 studs were carefully positioned on the machine axis using a cross-line laser level to ensure precise centering of the load application. Furthermore, the testing machine was equipped with a ball joint to guarantee even distribution of the applied load across both studs. The compression tests were carried out under displacement control at a rate of 2 mm/min.

In the tests, it was observed that the breakage was always produced in the stud, in the area of the weld collar, just at the beginning of the weld collar (see Fig. 9). The maximum load registered $F_{u,exp}$ for the studs tested under shear and the presence or not of a

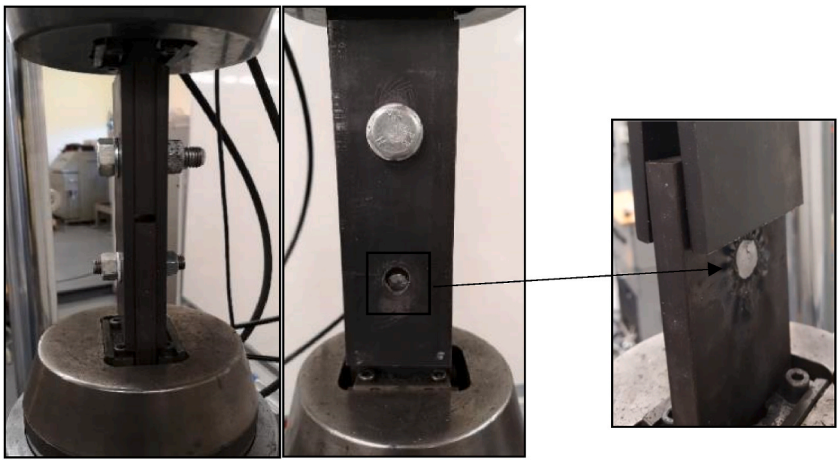

Fig. 9. Testing the specimen M16 (left) under shear and detail of the breakage of the studs (right).

counterbored hole is shown in Table 4. According to the tension tests results to determine the shear resistance of M16 studs, it has been observed that, for the same metric and grade of stud, the experimental load reached in the tests is very similar, with differences lower than 1.2%. Therefore, it is concluded that boring the hole to make it wider does not have significantly influence on the resistance of the studs under shear. For this reason, only two tests with counterbored holes were carried out for the M20 studs in the compression mode. Table 4 also shows the measured diameter of the weld collar, d_3, and the experimental ultimate shear stress ($\tau_{u,exp}$).

3. Analytical model of resistance

The moment resistance of the full joint under bending moments can be calculated from the resistance of the weakest basic component, according to (1).

$$M_R = F_R \cdot z \tag{1}$$

Where F_R is the resistance of the weakest basic component of the joint and z is the lever arm of the joint.

The following basic components were identified: studs (studs in tension, studs in shear, studs in combined tension and shear, punching shear in the frontal face of the column), flange cleat in bending and lateral face of the column under compression.

In addition to these components of which moment resistance is evaluated through equation (1), the failure of the lateral faces under shear (see point 3.4) should be assessed in a different way, by considering for the resistance the shear forces in the column below and above the beam-column connection. The use of equation (1) is only valid as a conservative approach for one-side beam-column joints. However, in the present research, like it happens in most common practical joints, it was observed that other component failures occur clearly before the failure of the lateral faces under shear.

The failure of the bolts connecting the beam flanges and the angle cleats should be studied like in conventional beam-column joints. However, since all the studied joints were designed with oversized prestressed bolts, the study of their slip, shear or bearing failure could be excluded from this research piece.

3.1. Resistance of welded studs

The resistance of the welded studs was calculated by adaption of the Eurocode 3.1.8 equations for bolts. The studs were calculated as subjected to different loading conditions: studs in tension, studs in shear, lamellar tearing of the studs, studs in combined tension and shear and punching shear in the frontal face of the column due to the studs.

The resistance of welded studs in tension, $F_{t,Rd}$, was calculated according to equation (2), where $f_{u,s}$ is the ultimate strength of the welded stud, A_s is the reduced area of the stud and γ_{M2} is the partial safety factor. In this study this factor has been assumed equal to one, while in the design standards the most common value is 1.25.

Table 4
Experimental ($F_{u,exp}$) and analytical ($F_{v,Rd}$) shear resistance of studs under shear.

Specimen	$F_{u,exp}$ [kN]	Hole	d_3 [mm]	$F_{v,exp}$ [kN]	$F_{v,Rd}$ [kN]	$\frac{F_{v,exp}}{F_{v,Rd}}$
S16–4.8	173	Counterbored	18.3	86.5	93.4	0.93
S16–4.8	175	Not counterbored	18.3	87.5	93.4	0.94
S16–K800	231	Counterbored	17.5	115.5	127.0	0.91
S16–K800	231	Not counterbored	17.7	115.5	129.9	0.89
S20–4.8	267	Counterbored	21.3	133.5	126.5	1.05
S20–K800	344	Counterbored	21.4	172.0	189.9	0.91

$$F_{t,Rd} = \frac{0.9 \cdot f_{u,s} \cdot A_s}{\gamma_{M2}} \tag{2}$$

The resistance of the frontal face of the column under punching shear, $B_{p,Rd}$, was calculated according to (3) where d_2 is the reduced diameter of the stud, t_0 is the thickness of the column, $f_{y,0}$ is the yield stress of the column and γ_{M2} is the partial safety factor. Again, this factor was assumed here equal to 1 in order to contrast with the experimental results.

$$B_{p,Rd} = \frac{0.6 \cdot \pi \cdot d_2 \cdot t_0 \cdot f_{y,0}}{\gamma_{M2}} \tag{3}$$

The resistance of the welded stud under laminar tearing, $F_{lt,Rd}$, was calculated according to (4), adapted from Maquoi et al. [19] where d_2 is the reduced diameter of the stud, $f_{y,0}$ is the yield stress of the column and γ_{M2} is the partial safety factor, assumed here equal to 1.

$$F_{lt,Rd} = 0.9 \frac{\pi \cdot d_2^2 \cdot f_{y,0}}{4 \cdot \gamma_{M2}} \tag{4}$$

The shear resistance of welded stud, $F_{v,Rd}$, was calculated according to equation (5) where a_v is a coefficient variable with the class of the stud. For studs where the shear plane passes through the threaded area: $a_v = 0.6$ for class 8.8 and $a_v = 0.5$ for class 4.8, while in the cases where the shear plane passes through the unthreaded area of the studs: $a_v = 0.6$. In equation (5) $f_{u,s}$ is the ultimate strength of the welded stud, A_s is the reduced area of the stud and γ_{M2} is the partial safety factor, once again assumed equal to 1.

$$F_{v,Rd} = \frac{a_v \cdot f_{u,s} \cdot A_s}{\gamma_{M2}} \tag{5}$$

The resistance of welded studs in combined tension and shear was calculated following equation (6) where $F_{v,Ed}$ is the applied shear, $F_{v,Rd}$ is the shear resistance of the stud, $F_{t,Ed}$ is the applied tension and $F_{t,Rd}$ is the tension resistance of the stud.

$$\frac{F_{v,Ed}}{F_{v,Rd}} + \frac{F_{t,Ed}}{1.4\, F_{t,Rd}} \leq 1 \tag{6}$$

3.2. Resistance of the flange cleat in bending

In bolted connections an equivalent T-stub in tension may be used to model the design resistance of the flange cleat in bending [29]. This design method has been proposed and validated by Ref. [30] and then has been included in Eurocode 3.8. The failure mode of a T-stub flange can occur in three different failure modes: mode 1 or complete yielding of the flange, mode 2 or bolt failure combined with yielding of the flange and mode 3 or bolt failure.

The design resistance of the T-stub flange under complete yielding of the flange (mode 1), $F_{T,1,Rd}$ was calculated by using equation (7) where $M_{pl,1Rd}$ is the moment when complete yielding of the flange occurs, and it can be calculated by (8) and m can be obtained from Fig. 5. The geometry factor 'm' takes into consideration the potential yielding of the angle cleat, which is dependent on the gap between the beam and the column. Yielding can occur either on the longer or shorter leg of the angle cleat. When the distance between the beam and the column exceeds 0.4 times the thickness of the angle cleat, yielding takes place on the longer leg. Conversely, when the distance is equal to or less than 0.4 times the thickness of the angle cleat, yielding occurs on the shorter leg. The detailed positions are described in Fig. 5.

$$F_{T,1,Rd} = \frac{4 \cdot M_{pl,1Rd}}{m} \tag{7}$$

$M_{pl,1,Rd}$ can be calculated with equation (8) assuming a T-stub equivalent with an effective length $l_{eff,1}$ equal to 0.5 times the length of the angle cleat, in which t_l is the thickness of the angle cleat, $f_{y,l}$ is the yield stress of the angle cleat and γ_{M0} is the partial safety factor.

$$M_{pl,1,Rd} = \frac{\sum l_{eff,1} \cdot t_l^2 \cdot f_{y,l}}{4 \cdot \gamma_{M0}} \tag{8}$$

The design resistance of the studs failure combined with yielding of the flange (mode 2), $F_{T,2,Rd}$ was calculated with equation (9). $M_{pl,2,Rd}$ is the moment that produces the yielding of the flange and can be calculated from (10), n is the distance from the stud-axis to the border of the leg of flange (Fig. 5), $F_{T,2}$ is the tension resistance of studs and m is as defined in Fig. 5.

$$F_{T,2,Rd} = \frac{2 \cdot M_{pl,2,Rd} + n \sum F_{t,Rd}}{m + n} \tag{9}$$

$M_{pl,2,Rd}$ can be calculated with equation (10) assuming a T-stub equivalent with an effective length $l_{eff,2}$ equal to 0.5 times the length of the angle cleat, t_l is the thickness of the angle cleat, $f_{y,l}$ is the yield stress of the angle cleat and γ_{M0} is the partial safety factor.

$$M_{pl,2,Rd} = \frac{\sum l_{eff,2} \cdot t_l^2 \cdot f_{y,l}}{4 \cdot \gamma_{M0}} \tag{10}$$

The resistance of the welded studs (mode 3) $F_{T,3,Rd}$ was calculated with equation (11) where $F_{T,Rd}$ is the resistance of individual welded studs.

$$F_{T,3,Rd} = \sum F_{t,Rd} \tag{11}$$

Finally, the design tension resistance of the T-stub flange can be calculated according to equation (12). It is important to notice that prying effects are implicitly taken into account when determining the design tension resistance of $F_{T,1,Rd}$, $F_{T,2,Rd}$, and $F_{T,3,Rd}$.

$$F_{T,Rd} = \min\left(F_{T,1,Rd}, F_{T,2,Rd}, F_{T,3,Rd}\right) \tag{12}$$

3.3. Resistance of the lateral face of the column in compression

The resistance of the lateral face of the column under compression ($F_{L,c,Rd}$) was calculated according to Eurocode 3, Part1.8 [28] recommendations for open-sections, but adapting the expressions to take into account the two lateral faces of the column. This methodology has been proposed in welded beam to columns joints and it has been validated by the authors in a previous work [9]. equation (13) is able to obtain the design resistance of the lateral face of the column in compression, where ω is a reduction factor to introduce the interaction between compression and shear. ω is variable with the transformation parameter β_T that can be obtained from table 5.4 in Eurocode 3, Part 1.8 [28]. ω can be calculated for different values of β_T according to equation (14). The coefficient ω_1 is obtained by equation (15) and the effective width of the lateral face by equation (16), where t_l and r_l are the thickness and radius of curvature of the angle cleat, A_v is the shear area of the column, t_0 is the thickness of the column, $f_{y,0}$ is the yield stress of the column and γ_{M0} is the safety factor taken as 1.

$$F_{L,c,Rd} = \frac{2 \cdot \omega \cdot b_{eff} \cdot t_0 \cdot f_{y,0}}{\gamma_{M0}} \tag{13}$$

$$\omega = \begin{cases} \omega_1, & if\ \beta_T = 1 \\ \omega_1 + 2(1-\beta_T)(1-\omega_1), & if\ 0.5 < \beta_T < 1 \end{cases} \tag{14}$$

where:

$$\omega_1 = \frac{1}{\sqrt{1 + 1.3 \cdot \left(\frac{2 \cdot b_{eff} \cdot t_0}{A_v}\right)^2}} \tag{15}$$

$$b_{eff} = 2t_l + 0.6r_l + 5(t_0 + 2.4t_0) \tag{16}$$

3.4. Resistance of the lateral face of the column in shear

The resistance of the column lateral face in shear $V_{L,Rd}$ was calculated according to the Eurocode 3, Part 1.8 [28] recommendations for open sections. equation (17), allows the column lateral face resistance in shear to be calculated, where A_v is the column shear area, $f_{y,0}$ is the column yield stress and γ_{M0} is the safety factor, taken as 1.

$$V_{L,Rd} = \frac{0.9 \cdot A_v \cdot f_{y,0}}{\sqrt{3} \cdot \gamma_{M0}} \tag{17}$$

3.5. Resistance of the column frontal face in bending

The resistance of the column front face in bending ($F_{f,Rd}$) was calculated by adaption of the expression proposed by Grotmann & Sedlacek [31] in the CIDET's project number 5BB-8/98.This equation was successfully applied by the authors to welded joints in a previous work [32]. equation (18) shows this proposal in which the effective length for one stud-row in tension L_{eff} can be calculated according to (19), where β is the ratio of the distance between the studs and the width of the column b_0, t_0 is the column thickness and $f_{y,0}$ is the yield stress of the column.

$$F_{f,Rd} = \frac{2 \cdot t_0^2 \cdot L_{eff} \cdot f_{y,0}}{b_0 \cdot (1-\beta)} \tag{18}$$

$$L_{eff} = 2 \cdot b_0 \cdot \sqrt{1-\beta} \tag{19}$$

4. Validation of the equations for the specific component: welded studs

Arc stud welding involves the same metallurgical principles found in any other arc welding process. In stud welding, the mechanical properties of welded studs are not constant along the edge [33], with yield stress and tensile strength varying along the weld, the Heat Affected Zones (HAZ) and the base materials. Equations (2) and (5) are an adaptation of the equations included in EC3 for bolts, in which the mechanical properties of bolts usually remain constant along the bolt. This section evaluates the agreement between the proposed analytical equations and the results obtained in tests in which welded studs were subjected to tension and shear.

4.1. Resistance of the welded studs in tension

Table 3 shows the analytical resistance of the welded stud in tension ($F_{t,Rd}$), calculated according equation (2), the resistance of the frontal face of the tube under punching shear, $B_{p,Rd}$, calculated according to equation (3), and the analytical resistance of the studs

under lamellar tearing, $F_{lt,Rd}$, which was calculated according to equation (4). The mechanical properties of the studs were taken from previous studies carried out by the authors [33] in which the mechanical properties of the studs once welded were obtained by means of indirect methods. The mechanical properties were taken from the welded zone. The resistance of the stud, $R_{s,Rd}$, as the minimum of $F_{t,Rd}$, $B_{p,Rd}$, $F_{lt,Rd}$ is also showed in the table.

From the table it is inferred that the analytical resistance of the studs can be calculated using the proposed equations with a good agreement, with most of the results on the safety side and an average global safety factor of 0.95 and an average absolute deviation (AAD) of 16%. However, in the case of considering the nominal properties of the materials, the average global safety factor will change to 1.29 and the AAD to 23%. Regardless of the properties considered in the analytical predictions, an early breakage of the stud has been observed in two cases where a M20 stud with qualities 4.8 and K800 was welded to a 6 mm thickness tube. The failure of the M20 stud under an experimental load lower than that of the equivalent M16 stud suggests that the welding did not achieve full resistance. Although the weld collar appeared to be evenly shaped, welding K800 class studs are more difficult than other studs grades and welding parameters should be kept within narrower limits. Although these parameters are correctly defined, in some cases [34] defects such as lack of fusion and porosity were found in the welds.

4.2. Resistance of the welded studs under shear

The analytical shear resistance, $F_{v,Rd}$ was calculated according to equation (5) and considering the mechanical properties of the welded studs that were determined by the authors in a previous study [32]. Good agreement was found between experimental and analytical shear resistance, with a maximum error of 13%, an AAD of 8.13% and an average safety factor of 0.94. This indicates that the shear resistance of the studs can be determined with common equations for the shear failure of bolts by considering as surface under shear the corresponding of the weld collar and the actual mechanical properties of the welded studs in that area. However, in practical design, the size of the weld collar is variable with welding parameters (current, time, lift, protusion and damping) and typically unknown at the design stage, with a diameter that can be smaller than the nominal one stated by the manufacturer in the data sheet (19.5 mm for M16 and 24.5 mm for M20 studs). Therefore, design shear resistance of studs using the nominal diameters of the weld collar is not a safe design practice (average safety factor of 0.77), and more conservative approaches, such as considering as the area under shear the nominal section of the stud (average safety factor of 1.45) or even the reduced section (average safety factor of 2.18) are preferable.

5. Discussion

The resistance of the basic components of the joint was assessed using equation (1), and subsequently, the components were arranged in ascending order based on their resistance. In the calculations, the mechanical properties of the welded studs were taken from previous studies carried out by the authors [33] in which the mechanical properties of the studs once welded were obtained by means of indirect methods. The specific resistance values are as follows: 643.1 MPa for M16 K800 studs joined with a 6- or 8-mm thickness hollow section, 538.5 MPa for M16 K800 studs joined with a 10-mm thickness hollow section. In the case of M16 4.8 studs, the nominal properties of the stud were used as the experimental values were not available. Table 5 presents the analytical moment resistance of the two components that exhibited the lowest levels of resistance, identified as $M_{R,an1}$ and $M_{R,an2}$. The table also includes the experimental moment resistance $M_{R,EXP}$ of the joints and the experimental failure modes.

The resistance of the joints ranged from 18 to 41 KNm. With respect to the experimental ultimate failure modes, the failure mode that produced the collapse of the joints formed by columns with 6-mm tube thickness was the punching shear of the frontal face at the studs-row subjected to tension (Fig. 10). However, in joints formed by columns with 8-mm or 10-mm tube thickness the failure mode that produced the collapse of the joint was the failure of the studs-row subjected to tension (Fig. 10). As it can be seen in Fig. 10, the breakage of the stud occurred in the reduced diameter section of the stud, i.e., in the unthreaded area of the stud. The ultimate failure was preceded by a noticeable deformation of the frontal face of the column in some cases, while in other cases the collapse came after a noticeable deformation of the angle cleats. Fig. 11 shows the deformations observed during the tests for the joints SMS1 to SMS6. In the

Table 5
Analytical results. Experimental moment resistance ($M_{R,EXP}$), experimental failure mode, first ($M_{R,an1}$) and second ($M_{R,an2}$) analytical moment resistance and first and second analytical failure modes.

Joint	$M_{R,EXP}$ [kNm]	EXP Failure mode	$M_{R,an1}$ [kNm]	1st Failure mode (an1)	$M_{R,an2}$ [kNm]	2nd Failure mode (an2)
SMS1	22.14	P	21.47	CF	24.81	P
SMS2	34.71	S	34.17	C	36.45	P
SMS3	31.66	S	31.72	S (T)	32.61	C
SMS4	30.37	P	22.57	CF	34.72	P
SMS5	40.99	S	36.36	C	44.70	CF
SMS6	41.34	S	36.36	C	42.53	S (V + T)
SMS7	38.02	P	25.87	CF	34.26	P
SMS8	36.61	S	36.36	C	50.94	S (V + T)
SMS9	38.51	S	36.36	C	42.67	S (V + T)
DMS1	17.94	S	21.06	S (V + T)	23.56	S (T)
DMS2	31.68	P	22.52	CF	25.74	S (V + T)
DMS3	26.28	S	25.75	S (V + T)	32.94	S (T)
DMS4	29.03	S	25.75	S (V + T)	32.94	S (T)

Notation: P: punching shear, CF: column frontal face, C: angle cleat, S: stud, T: tension, V: shear.

Fig. 10. Failure modes. Example of punching shear of frontal face at the studs-row in tension for joint SMS1 (left) and failure mode of the studs-row subjected to tension in joint SMS5 (right).

Fig. 11. Deformations observed during the tests for the specimens SMS1 to SMS6.

SMS1 and SMS4 specimens, a noticeable deformation of the frontal face of the tube is observed, while the deformation of the flange of the angle cleat subjected to tension is observed for the rest of the joints. These deformations remained after the joint breakage, suggesting the yielding of these components.

From the analytical results it can be inferred that for specimens SMS2, SMS5, SMS6, SMS8 and SMS9 the first analytical mode of failure was on the flange of the angle cleat in bending (C). When the joint is assembled with a column with thickness of $t_0 = 6$ mm (joints SMS1, SMS4, SMS7 and DMS2) the first mode of failure was produced by the failure of the frontal face of the column (CF). For the rest of joints, the first mode of failure is produced by the failure of the studs under tension (T) or under a combination of tension and shear (V + T).

To proceed with a fair comparison between experimental and analytical results it is important to take into account that from the experiments, the observed ultimate failure mode was punching or a failure on the stud. Therefore, Table 6 shows the experimental moment resistance of the tested joints together with the analytical moment resistance but without considering those analytical results in which the failure was on the angle cleat or on the frontal face of the tube showed in Table 5, that is, taking only into account the

Table 6
Analytical results. Experimental moment resistance ($M_{R,EXP}$), experimental failure mode, analytical moment resistance $M_{R,an}$ and analytical failure mode.

Joint	$M_{R,EXP}$ [kNm]	Ultimate failure mode EXP	$M_{R,an}$ [kNm]	Failure mode	$\frac{M_{R,EXP}}{M_{R,an}}$
SMS1	22.14	P	24.81	P	0.89
SMS2	34.71	S	36.45	P	0.95
SMS3	31.66	S	31.72	S	1.00
SMS4	30.37	P	34.72	P	0.87
SMS5	40.99	S	50.86	S (V + T)	0.81
SMS6	41.34	S	42.53	S (V + T)	0.97
SMS7	38.02	P	34.26	P	1.11
SMS8	36.61	S	50.94	S (V + T)	0.72
SMS9	38.51	S	42.67	S (V + T)	0.90
DMS1	17.94	S	21.06	S (V + T)	0.85
DMS2	31.68	P	25.74	S (V + T)	1.23
DMS3	26.28	S	25.75	S (V + T)	1.02
DMS4	29.03	S	25.75	S (V + T)	1.13

Notation: P: punching shear, S: stud, T: tension, V: shear.

punching failure or the studs failure. From the data shown in Tables 6, it can be seen that the analytical modelling of the joint resistance reproduces the predicted failure modes and the moment resistance acceptably. In two joints (SMS2 and DMS2 specimens), the failure mode was not correctly predicted. However, in the case of the SMS2 specimen, punching shear failure (equation (3)) occurs analytically at 36.45 kNm, while the analytical tensile failure of the studs (equation (2)) occurs at 37.88 kNm. This suggests that punching failure and tensile failure occur almost simultaneously, in accordance with the analytical proposal and in close proximity to the experimental result.

In Fig. 12 the analytical moment resistance ($M_{R,an}$) have been plotted against the experimental moments ($M_{R,EXP}$). In the figure the dashed lines indicate a ±20% deviation. According to the data shown in the figure, a good agreement is observed between the analytical predictions and the experimental results, with maximum discrepancies of 18.73% for the DMS2 specimen and an average absolute deviation of 9.01%. The results were better fitted when only the results of the SMS specimens (mean absolute error of 7.52%) are considered compared to the DMS specimens (mean absolute error of 12.37%).

According to the Eurocode 3 classification of joints by strength, all the SMS and DMS joints with the exception of SMS7, can be classified as nominally pinned due to the fact that the design moment resistance of these joints is not higher than 0.25 times the design moment resistance of the connected members. This means that joints with welded studs can transmit the internal forces, without developing significant moments. SMS 7 joint was classified as a partial-strength joint. Although these joints could be simply classified according to their strength, their demonstrated low-semi-rigid behaviour in terms of stiffness [25] means that in the global structural analysis of the frame, the joints will be working under low moments. Depending on the structural design, the moments obtained from the overall analysis may be low enough to be adequately resisted by these types of joints.

Despite the possibility of this simple classification according to strength, the proved low-semi-rigid behaviour of these joints according to stiffness [25] will make them support very limited moments in the corresponding semi-rigid frames. These moments obtained from the global analysis could be low enough (depending on the structural design) to be effectively resisted by this type of joints.

5.1. Studying the resistance of untested joints

Once the analytical model of resistance was validated with the experimental results, it was used to study the resistance of 18 untested geometries of joints denoted as FEBC01 to FEBC18. The studied joints were chosen considering geometries of the connected members that allows the joint to be assembled easily, i.e., the column is width enough to weld two studs in a row and the beam has approximately the same width as the column. For a practical purpose, the joints studied are the expected to be required in the design of low-rise and medium-rise residential steel buildings.

The studied beam-to-column joints are presented in Table 7 and consisted of IPE beams connected to SHS columns with a steel grade of S275. The joints were designed with two different angle cleats of L120 × 80 × 10 and L120 × 80 × 12. The threaded studs were chosen with a diameter of 20 mm, with a reduced unthreaded area and class of K800.

From Table 7 it is inferred that the failure of joints formed by columns with 6-mm thickness is due to the yielding of the frontal face, independently of the angle cleat thickness. When the joint is formed by an 8-mm or 10-mm thickness column in combination with a 10-mm angle cleat thickness, the failure mode is due to the yielding of the angle cleat. In the rest of joints formed with a 12-mm angle cleat thickness, the failure mode is due to the yielding of the angle cleat or due to the punching shear of the stud, depending on the thickness of the column and the length of the angle cleats.

The moment resistance of the joints revealed the effect of increasing the thickness of the angle cleat. For joints in which the resistance is governed by the failure of the frontal face (joints formed by columns with a thickness of 6 mm) the moment resistance of the joints hardly changes with higher thickness in the angle cleat. However, in joints in which the failure is governed by the angle cleat (joints formed by columns with 8- or 10-mm thickness) the moment resistance increases in a range of 12% to 37%, with an average rate of growth of 30%.

The untested joints were also classified by strength according to Eurocode 3 rules. The results were that joints FEBC03, FEBC06, FEBC07, FEBC08, FEBC09, FEBC12, FEBC13, FEBC15, FEBC18 with 10-mm angle cleats were classified as nominally pinned joints.

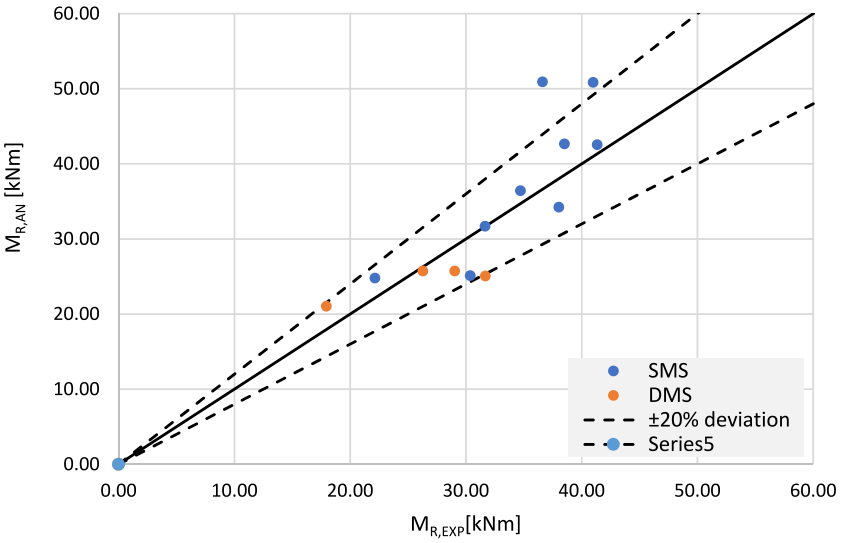

Fig. 12. Assessment of beam to column resistance analytical approach.

Table 7
Analytical moment resistance $M_{R,an}$, and predicted analytical failure mode in untested joints formed by 10 mm and 12 mm angle cleats.

Joint	Beam IPE	Column SHS	t_l = 10 mm		t_l = 12 mm	
			$M_{R,an}$ [kNm]	Failure mode	$M_{R,an}$ [kNm]	Failure mode
FEBC01	240	120 × 6	20.96	CF	21.03	CF
FEBC02	240	120 × 8	22.18	C	35.39	C
FEBC03	240	120 × 10	22.18	C	35.39	C
FEBC04	270	140 × 6	23.39	CF	23.46	CF
FEBC05	270	140 × 8	27.58	C	41.61	P
FEBC06	270	140 × 10	27.58	C	43.99	C
FEBC07	300	160× 6	25.81	CF	25.88	CF
FEBC08	300	160 × 8	33.56	C	45.56	P
FEBC09	300	160 × 10	33.56	C	53.52	C
FEBC10	330	160 × 6	31.56	CF	31.64	CF
FEBC11	330	160 × 8	38.92	C	49.51	P
FEBC12	330	160 × 10	38.92	C	61.89	P
FEBC13	360	175 × 6	33.41	CF	33.49	CF
FEBC14	360	175 × 8	44.66	C	53.46	P
FEBC15	360	175 × 10	44.66	C	66.83	P
FEBC16	400	180 × 6	39.58	CF	39.67	CF
FEBC17	400	180 × 8	51.95	C	58.73	P
FEBC18	400	180 × 10	51.95	C	73.41	P

Notation: P: punching shear, CF: column frontal face, C: angle cleat.

With respect to the joints formed by 12 mm angle cleats, those coded as FEBC06 and FEBC12 were also classified as nominally pinned. The rest of joints (half of the group with angle cleat of 10-mm thickness and most of the joints with angle cleat of 12-mm thickness) were classified as partial-strength joints. As it was mentioned in the previous section, this classification according to strength does not have to be definitive if a more detailed structural analysis is carried out, since these joints act as semi-rigid with low initial stiffness. This leads the joints of conventional frames to develop low moment that, in most cases, could be resisted by the proposed connection.

6. Design of joints with welded studs

According to the results of the analytical model, the behaviour of the considered beam-to-column joints with welded studs is governed by the yielding of the frontal face of the tube or by the deformation of the angle cleats, being the collapse of the joint due to the punching shear of the frontal face of the tube at the row of studs in tension or due to the failure of studs. The dimensions of the column thickness, the thickness of the angle cleats and the diameter of studs govern the main behaviour of the full joint.

When an early failure of studs occurs, the joints have a brittle fracture with no plastic deformation prior to failure. This may lead to joints with welded studs to have no ductility enough to be suitable for the design of residential steel buildings. However, with an efficient design of joints with welded studs, this behaviour can be avoided. In this section, some equations are proposed to achieve effectively designs of beam-to-column joints with angle cleats and welded studs.

6.1. Behaviour of the joint governed by angle cleats

The behaviour of a joint is governed by the deformation of the angle cleats, offering a high rotation capacity and being assimilated to unlimited rotation capacity (plastic hinge) when satisfies the condition shown in equation (20) [35]. In this equation t_l is the thickness of the angle cleat, d_2 is the reduced diameter of the stud, $f_{u,s}$ is the ultimate strength of the stud and $f_{y,l}$ is the yield stress of the angle cleat. Joints that satisfy equation (21) are joints that show reduced or limited plastic rotation capacity, but they can reach the design moment resistance without brittle fracture. In this intermediate case, a plastic verification of the angle cleat can be done. The joints that meet (22) present insufficient deformation capacity.

$$\text{Unlimited rotation capacity} \rightarrow t_l \leq 0.36 \cdot d_2 \sqrt{\frac{f_{u,s}}{f_{y,l}}} \tag{20}$$

$$\text{Limited rotation capacity} \rightarrow 0.36 \cdot d_2 \sqrt{\frac{f_{u,s}}{f_{y,l}}} < t_l < 0.53 \cdot d_2 \sqrt{\frac{f_{u,s}}{f_{y,l}}} \tag{21}$$

$$\text{Insufficient rotation capacity} \rightarrow t_l \geq 0.53 \cdot d_2 \sqrt{\frac{f_{u,s}}{f_{y,l}}} \tag{22}$$

6.2. Behaviour of the joint governed by frontal face

The behaviour of a joint is governed by the deformation of the column face, offering a high rotation capacity and being assimilated to unlimited rotation capacity (plastic hinge) when meets the criteria outlined in equation (23). In this equation t_0 is the thickness of the column, d_2 is the reduced diameter of the stud, $f_{u,s}$ is the ultimate strength of the stud and $f_{y,0}$ is the yield stress of the column. Joints that satisfy equation (24) are joints that shows reduced or limited plastic rotation capacity, but they can reach the design moment resistance without brittle fracture. The joints that meet (25) present insufficient deformation capacity.

$$\text{Unlimited rotation capacity} \rightarrow t_0 \leq 0.36 \cdot d_2 \sqrt{\frac{f_{u,s}}{f_{y,0}}} \tag{23}$$

$$\text{Limited rotation capacity} \rightarrow 0.36 \cdot d_2 \sqrt{\frac{f_{u,s}}{f_{y,0}}} < t_0 < 0.53 \cdot d_2 \sqrt{\frac{f_{u,s}}{f_{y,0}}} \tag{24}$$

$$\text{Insufficient rotation capacity} \rightarrow t_0 \geq 0.53 \cdot d_2 \sqrt{\frac{f_{u,s}}{f_{y,0}}} \tag{25}$$

From equations (20) and (23) the maximum thickness of the angle cleats and the maximum thickness of the frontal face of the column can be calculated to design of joints with unlimited rotation capacity. Table 8 provide guidelines for designing joints with unlimited rotation capacity for different steel grades of the column and for various grades and metric of RD studs.

From the table it can be inferred that when using M20 K800 RD studs in combination with 10 mm angle cleats and columns of 6 mm thickness, the rotation capacity is near to unlimited. However, when combining M20 K800 RD studs with 12 mm angle cleats thickness, the rotation capacity changes to limited rotation capacity.

7. Conclusions

The advantages of designing bolted joints in buildings with welded studs are their expected ability to be disassembled, guaranteeing their capacity to change location, their capacity to be assembled quickly, their capacity to achieve an efficient separation of components and materials for their recovery and reducing the execution costs associated to traditional welded joints. Based on the above commented advantages it can be stated that this kind of joints contributes to a more efficient, environmentally friendly, and sustainable construction.

In this paper, the resistance of demountable bolted joints connecting IPE beams to hollow section columns based on welded studs

Table 8
Maximum thickness of the angle cleats ($t_{l,max}$) and maximum thickness of the column ($t_{0,max}$) to reach unlimited rotation capacity.

Column grade	Threaded RD stud	Stud grade	$t_{l,max}$ [mm]	$t_{0,max}$ [mm]
S275	M16	4.8	5.8	6.3
		K800	7.3	7.9
	M20	4.8	7.4	8,0
		K800	9.3	10.0
S355	M16	4.8	5.8	5.5
		K800	7.3	6.9
	M20	4.8	7,4	7.0
		K800	9.3	8.8

has been examined by means of experimental tests and simplified analytical models. In the models, the basic components of the joint were identified, according with the component method, and their individual resistance was determined allowing the behavioural resistance of the full joint to be quantified. The analytical models were validated by comparison with the corresponding experimental results and later the model was extended to obtain the resistance of other beam-column joint combinations that are appropriate to be used in low-rise and medium-rise residential steel buildings. From this research, some more specific conclusions and design guidelines for the joints are now outlined.

1) The resistance of this kind of joint is mainly governed by three design parameters: the thickness of the column, the thickness of the angle cleats and the diameter and grade of the studs.
2) When designing joints with a thin column, the behaviour of the joint is governed by the yielding of the frontal face while their collapse is produced by the punching shear of the frontal face of the column at the row of the studs under tension.
3) When designing joints with a thicker column, the behaviour of the joint is governed by the angle cleats, while their collapse is produced by the breakage of the studs.
4) The resistance of the studs was evaluated by using equations for bolts. In the calculations, the mechanical properties of the welded zones were used in combination with the reduced diameter of the studs. When using these mechanical properties, the results obtained were close to the experimental values.
5) The influence of the angle cleat thickness in the moment resistance of the full joint has also been studied. Thus, those joints in which the failure is governed by yielding of the frontal face of the tube, the resistance remains constant for both angle cleat thicknesses considered (10 mm and 12 mm). However, when the failure of the joint is governed by the angle cleats, the moment resistance of the joint increases by an average of 30% using thicker angle cleats.
6) A new component-based analytical model for strength, able to reproduce both failure modes and resistance moments of the joints has been proposed. Then, new component characteristics have been proposed for the key components of the tube. This confirms that when considering the key components of the tube, the component method can be extended to joints formed by hollow sections.
7) Easily removable joints must be designed with tight tolerances to be removable by hand. However, joints formed by 6 mm thickness columns presents a noticeable deformation of their frontal face when the yield is exceeded. Further investigations must be done in order to this deformation be quantified to ensure an easy re-assembly of their components.
8) A set of guidelines has been proposed for designing joints with welded studs. The equations presented allows the maximum thickness of the angle cleat to be determined based on the expected behavior of the full joint.

Author statement

Ismael García: Conceptualization, Methodology, Formal analysis, Investigation, Writing - Original Draft **Miguel A. Serrano**: Conceptualization, Resources, Writing - Review & Editing, Project administration, Funding acquisition **Carlos López-Colina**: Conceptualization, Methodology, Formal analysis, validation, Writing - Review & Editing **Fernando L. Gayarre:** Resources.

Declaration of competing interest

The authors declare that they have no known competing financial interests or personal relationships that could have appeared to influence the work reported in this paper.

Data availability

Data will be made available on request.

Acknowledgements

The authors would like to acknowledge the financial support provided by the Spanish Ministry of Economy and Competitiveness through project BIA2017-83467-P, pre-doctoral grant PRE2018-084273 and by CIDECT through project 5CF. They would also like to thank the IEMES Research Group from the University of Oviedo for their support.

References

[1] D. 2010/31/CE, Directive 2010/31/EU of the European Parliament and of the Council of 19 May 2010 on the Energy Performance of Buildings, 2010.
[2] J. Deja, A. Uliasz-Bochenczyk, E. Mokrzycki, CO2 emissions from polish cement industry, Int. J. Greenh. Gas Control 4 (4) (2010) 583–588, https://doi.org/10.1016/j.ijggc.2010.02.002.
[3] World Steel Association, Steel's contribution to a low carbon future and climate resilient societies, World Steel Assoc 1–6 (2017).
[4] E. Benhelal, E. Shamsaei, M.I. Rashid, Challenges against CO2 abatement strategies in cement industry: a Review, J. Environ. Sci. (China) 104 (2021) 84–101, https://doi.org/10.1016/j.jes.2020.11.020.
[5] M. Marzouk, N. Elshaboury, Science mapping analysis of embodied energy in the construction industry, Energy Rep. 8 (2022) 1362–1376, https://doi.org/10.1016/j.egyr.2021.12.049.
[6] K.T. Adams, M. Osmani, T. Thorpe, J. Thornback, Circular Economy in construction: current awareness, challenges and enablers, Proc. Inst. Civ. Eng. Waste Resour. Manag. 170 (1) (2017) 15–24, https://doi.org/10.1680/jwarm.16.00011.
[7] L.H. Lu, J. Wardenier, Ultimate deformation criteria for uniplanar connections between I-beam and RHS columns under in-plane bending, in: Proceedings of the International Offshore and Polar Engineering Conference, 1994.
[8] L.H. Lu, The Static Strength of I-Beam to Rectangular Hollow Section Column Connections 5AX-6/98, 1998.

[9] C. López-Colina, M.A. Serrano, M. Lozano, F.L. Gayarre, J.M. Suárez, T. Wilkinson, Characterization of the main component of equal width welded I-Beam-to-RHS-Column connections, Steel Compos. Struct. (2019), https://doi.org/10.12989/scs.2019.32.3.337.
[10] T. O'Grady, R. Minunno, H.Y. Chong, G.M. Morrison, Design for disassembly, deconstruction and resilience: a circular Economy index for the built environment, Resour. Conserv. Recycl. 175 (May) (2021), 105847, https://doi.org/10.1016/j.resconrec.2021.105847.
[11] P. Rode, R. Burdett, J.C. Soares Gonçalves, Buildings: investing in energy and resource efficiency, Sustain. Dev. 19 (2011) 49–59, https://doi.org/10.1002/sd.
[12] J.K.W. Wong, J. Zhou, Enhancing environmental sustainability over building life cycles through green BIM: a Review, Autom. ConStruct. 57 (2015) 156–165, https://doi.org/10.1016/J.AUTCON.2015.06.003.
[13] C. Málaga-Chuquitaype, A.Y. Elghazouli, Component-based mechanical models for blind-bolted angle connections, Eng. Struct. (2010), https://doi.org/10.1016/j.engstruct.2010.05.024.
[14] A.Y. Elghazouli, C. Málaga-Chuquitaype, J.M. Castro, A.H. Orton, Experimental monotonic and cyclic behaviour of blind-bolted angle connections, Eng. Struct. (2009), https://doi.org/10.1016/j.engstruct.2009.05.021.
[15] C. Málaga-Chuquitaype, A.Y. Elghazouli, Behaviour of combined channel/angle connections to tubular columns under monotonic and cyclic loading, Eng. Struct. (2010), https://doi.org/10.1016/j.engstruct.2010.02.008.
[16] Y. Liu, C. Málaga-Chuquitaype, A.Y. Elghazouli, Response and component characterisation of semi-rigid connections to tubular columns under axial loads, Eng. Struct. 41 (2012) 510–532, https://doi.org/10.1016/j.engstruct.2012.03.061.
[17] Y. Liu, C. Málaga-Chuquitaype, A.Y. Elghazouli, Behaviour of beam-to-tubular column angle connections under shear loads, Eng. Struct. 42 (2012) 434–456, https://doi.org/10.1016/j.engstruct.2012.04.027.
[18] Y.C. Wang, L. Xue, Experimental study of moment-rotation characteristics of reverse channel connections to tubular columns, J. Constr. Steel Res. (2013), https://doi.org/10.1016/j.jcsr.2013.03.006.
[19] R. Maquoi, X. Naveau, Beam-Column Welded Stud Connections 5AG 83/5 (1983).
[20] R. Maquoi, X. Naveau, J. Rondal, Beam-column welded stud connections, J. Constr. Steel Res. (1984), https://doi.org/10.1016/0143-974X(84)90032-4.
[21] D. Vandegans, Liaison Entes Poutres Métalliques et Colonnes En Profils Creux Remplis de Béton, Basée Sur La Technique Du Goujonnage (Goujons Filetés). MT193. CRIF, 1995.
[22] D. Vandegans, Use of threaded studs in joints between I-beam and RHS-column, in: Istanbul Colloquium on Semi-rigid Connections; IABSE, Zürich, Switzerland, 1996, pp. 53–62.
[23] D. Vandegans, J. Janss, Connection between steel beams and concrete filled R.H.S. Based on the stud technique (threaded stud), Connect. Steel Struct. III (1996) 67–76, https://doi.org/10.1016/B978-008042821-5/50066-3.
[24] L.C. Neves, L. Simões da Silva, da S. Vellasco, P. C. G, Experimental behaviour of end plate I-beam to concrete-filled rectangular hollow section column joints, Adv. Steel Struct. (ICASS '02) (2002) 253–260, https://doi.org/10.1016/B978-008044017-0/50029-9.
[25] M.A. Serrano-López, C. López-Colina, Y.C. Wang, M. Lozano, I. García, F.L. Gayarre, An experimental study of I beam-RHS column demountable joints with welded studs, J. Constr. Steel Res. 182 (2021), 106651, https://doi.org/10.1016/j.jcsr.2021.106651.
[26] M.A. Serrano, C. López-Colina, Y.C. Wang, M. Lozano, F. López-Gayarre, I beam-RHS column joints with welded studs, in: 9th International Conference on Steel and Aluminium Structures (ICSAS19), Independent Publishing Network, Bradford, 2019, pp. 849–860.
[27] I. García, M.A. Serrano, C. López-Colina, F.L. Gayarre, The stiffness of beam-to-RHS joints with welded studs, J. Build. Eng. 70 (2023) 106340, https://doi.org/10.1016/j.jobe.2023.106340.
[28] EN 1993-1-8:2005, Eurocode 3: Design of Steel Structures - Part 1-8: Design of Joints. Eurocode 3, 2005.
[29] C. Faella, V. Piluso, G. Rizzano, Structural Steel Semirigid Connections: Theory, Design, and Software, CRC Press, 2000.
[30] P. Zoetemeijer, Design method for the tension side of statically loaded, bolted beam-to-column connections, Heron 20 (1) (1974).
[31] D. Grotmann, G. Sedlacek, Rotational Stiffness of Welded RHS Beam-To-Column Joints, CIDECT Project Number 5BB-8/98, 1998.
[32] M. Lozano, The component method applied to welded beam-column joints between open profiles and structural tubes, Doctoral Thesis, in: Spanish. Original Title: El Método de Los Componentes Aplicado a Uniones Viga-Pilar Soldadas Entre Perfiles Abiertos y Tubo Estructural, 2019.
[33] I. García, M.A. Serrano, C. López-colina, F.L. Gayarre, J.M. Suárez, Approaches to the mechanical properties of threaded studs welded to RHS columns, Materials (2021), https://doi.org/10.3390/ma14061429.
[34] Ungermann, D.; Schneider, S.; Trillmich, R. Tension Tests on Welded Threaded Studs with a Tensile Strength of 800N/Mm2.
[35] J.P. Jaspart, K. Weynand, Design of joints in steel and composite structures. https://doi.org/10.1002/9783433604762, 2016.